Available online at www.sciencedirect.com

ScienceDirect

www.elsevier.com/locate/jes

JES JOURNAL OF ENVIRONMENTAL SCIENCES

www.jesc.ac.cn

Response surface method for modeling the removal of carbon dioxide from a simulated gas using water absorption enhanced with a liquid-film-forming device

Diem-Mai Kim Nguyen[1], *Tsuyoshi Imai*[2,*], *Thanh-Loc Thi Dang*[3], *Ariyo Kanno*[2], *Takaya Higuchi*[2], *Koichi Yamamoto*[2], *Masahiko Sekine*[2]

1. *Graduate School of Environmental Sciences and Engineering, Yamaguchi University, Yamaguchi 755-8611, Japan*
2. *Graduate School of Sciences and Technology for Innovation, Yamaguchi University, Yamaguchi 755-8611, Japan*
3. *Department of Environmental Science, College of Sciences, Hue University, Hue 470000, Vietnam*

ARTICLE INFO

Article history:
Received 27 November 2016
Revised 17 March 2017
Accepted 20 March 2017
Available online 29 March 2017

Keywords:
Carbon dioxide
Water dissolution
Liquid-film
Response surface method (RSM)

ABSTRACT

This paper presents the results from using a physical absorption process to absorb gaseous CO_2 mixed with N_2 using water by producing tiny bubbles *via* a liquid-film-forming device (LFFD) that improves the solubility of CO_2 in water. The influence of various parameters—pressure, initial CO_2 concentration, gas-to-liquid ratios, and temperature—on the CO_2 removal efficiency and its absorption rate in water were investigated and estimated thoroughly by statistical polynomial models obtained by the utilization of the response surface method (RSM) with a central composite design (CCD). Based on the analysis, a high efficiency of CO_2 capture can be reached in conditions such as low pressure, high CO_2 concentration at the inlet, low gas/liquid ratio, and low temperature. For instance, the highest removal efficiency in the RSM–CCD experimental matrix of nearly 80% occurred for run number 20, which was conducted at 0.30 MPa, CO_2 concentration of 35%, gas/liquid ratio of 0.71, and temperature of 15°C. Furthermore, the coefficients of determination, R^2, were 0.996 for the removal rate and 0.982 for the absorption rate, implying that the predicted values computed by the constructed models correlate strongly and fit well with the experimental values. The results obtained provide essential information for implementing this method properly and effectively and contribute a promising approach to the problem of CO_2 capture in air pollution treatment.

Introduction

Global warming and climate change, with their numerous adverse effects on the weather, glaciers, sea level, wildlife, and human health, have attracted growing concern. Reducing the greenhouse effect, which is associated with the high concentration of greenhouse gases in the atmosphere, is now a global pursuit. Among the greenhouse gases, CO_2 constitutes a major proportion, at over 80% of the total greenhouse gas emissions (Lee et al., 2012). CO_2 alone accounts for about 64% of the warming effect caused by all greenhouse gases (Mondal et al., 2012; Yu et al., 2012; Ma'mun et al., 2007).

With the rapid growth of commerce and modern civilization, the world has ever-increasing energy demands that result in large CO_2 emissions. The atmospheric concentration of CO_2 has

* *Corresponding author*. E-mail imai@yamaguchi-u.ac.jp (Tsuyoshi Imai).

http://dx.doi.org/10.1016/j.jes.2017.03.026

increased more than 40% since the beginning of the industrial revolution (270–400 ppmV) and has been rising annually by 2 ppmV (Moreira and Pires, 2016; Singh and Ahluwalia, 2013). With industrial activities such as fossil fuel burning and industrial production, 30 billion tons of CO_2 are released to the atmosphere each year (Moreira and Pires, 2016; Li et al., 2013). In addition, according to the International Panel on Climate Change (IPCC), the atmospheric CO_2 concentration is predicted to increase to 936 ppmV before 2100 and lead to a rise in the mean global temperature of approximately 1.0–3.0°C (Chou, 2013; Lee et al., 2012). Therefore, removal of CO_2 from the atmosphere has recently become an urgent issue that has gained global attention, in order to mitigate global warming and the subsequent negative consequences.

Various technologies have been used to remove CO_2 from gas streams, *e.g.*, absorption, adsorption, membrane separation, cryogenic separation, and hydrate-based separation. Among the technologies mentioned above, absorption is the most widely used method to capture CO_2 from gas streams, because it is a well-established technique that has been in use for nearly 60 years (Babu, 2014; Rao and Rubin, 2002). The main principle of this method is to transfer one or more substances from a gas stream into a liquid phase through the vapor–liquid phase boundary.

There are two main types of absorption processes: physical absorption and chemical absorption. This classification is based on whether or not a chemical reaction occurs after the dissolution of substances into a liquid absorbent (Aresta, 2013). Chemical absorption using an amine solution is widely applied for the separation of CO_2 from exhaust gases, because of its high CO_2 removal efficiency. Even so, there remain several limitations in using this method. First, absorption using organic amines necessitates high energy consumption owing to the high temperature required during absorbent regeneration. Second, this method results in high corrosion and generates volatile degradation compounds. Moreover, amine emissions can degrade into nitrosamines and nitramines (Leung et al., 2014), which endanger human health and the environment. This method, therefore, is not environmentally friendly. On the other hand, these problems can be avoided by using a physical absorption process. In contrast to chemical absorption, the operation of physical absorption is based on Henry's law, which implies that the absorption process is temperature and pressure dependent and the removal of CO_2 depends on its solubility in the liquid phase (Olajire, 2010). Water absorption is one of the most popular processes for physical absorption. The fundamental principle of this method relies on the solubility of CO_2 in water. The separation of CO_2 from a gas stream occurs due to the difference in the solubility between CO_2 and other gases. CO_2 is more soluble in water than other gases, such as N_2, O_2, H_2, and CH_4 (Weiss, 1974). As a consequence, it can be absorbed in water more easily and thus removed from the feed streams. Through this method, absorption and desorption can be accomplished using water, which results in lower cost (for solvents and regeneration) and higher stability, all with an environmentally friendly process (resulting in no unexpected toxic by-products) (Xiao et al., 2014). However, this scheme retains the challenge of improving the CO_2 removal efficiency because of the lower interaction between CO_2 and water than when organic solvents are used for physical or chemical absorption. This method has not been applied widely and is in need of more research and development. In order to augment the solubility of gases in the aqueous phase, it is possible to form a liquid-film through the use of gas bubbles—especially fine bubbles or microbubbles—to produce a high interfacial area and enhance the interaction between gas molecules and liquids (Bang et al., 2014; Parmar and Majumder, 2013; Xu et al., 2008; Imai and Zhu, 2011).

Microbubbles are defined as tiny bubbles with diameter below 100 μm (Parmar and Majumder, 2013). Tiny bubbles have a high surface tension, small buoyancy, and low slip velocity, all of which leads to a longer residence time for gas bubbles in an aqueous solution. Microbubbles also have a high gas dissolution rate because the surface area and internal pressure of the bubble rise notably, resulting in an increase in the partial pressure of the dissolving gas and a decrease in the bubble rising speed (Parmar and Majumder, 2013). In addition, a large surface area can be provided per unit volume of gas. These properties of microbubbles support their use as a potential solution for improving the dissolution of CO_2 in a liquid phase.

The aim of this study is to implement our method of utilizing tap water as a solvent in conjunction with a liquid-film-forming device (LFFD) that is able to form microbubbles to promote the dissolution of CO_2 in the tap water. The general objective of this study is therefore to remove CO_2 from a mixed gas at high removal efficiency *via* an eco-friendly method to prevent the release of hazardous by-products. The response surface method (RSM) was used to build models for this absorption process that can be used as a beneficial tool in predicting and selecting optimum conditions.

1. Materials and methods

1.1. Materials

The simulated gas consisted of a mixture of nitrogen and CO_2 mixed by using gas flow meters. The CO_2 (99.99%) and N_2 (99.99%) gases were purchased from Iwatani Corporation (Japan). Tap water was employed directly as the once-through physical absorbent without any purification process.

1.2. Experimental apparatus and methods

The apparatus used in this study are shown in Fig. 1. The reactor is the main component of this system (represented as number 6 in Fig. 1), with 22 cm diameter and 16 cm height. The absorption reactor was designed to connect with the LFFD inside it, which has a 17 cm height and an 8 cm diameter, to generate large quantities of microbubbles.

The experiments were carried out at differing conditions of pressure, temperature, gas-to-liquid ratio (G/L), and initial CO_2 concentration. In this study, the inlet gas pressure was examined in the range of 0.25–0.75 MPa. The concentration of CO_2 mixed with N_2 was adjusted from 10% to 45% using a mass flow controller. Meanwhile, the G/L ratio was controlled by holding the liquid flow rate at 14 L/min while changing the gas flow rate from 5 to 25 L/min. Temperature was investigated in the range of 10°C to 30°C, which corresponds to the normal annual temperature range in Japan.

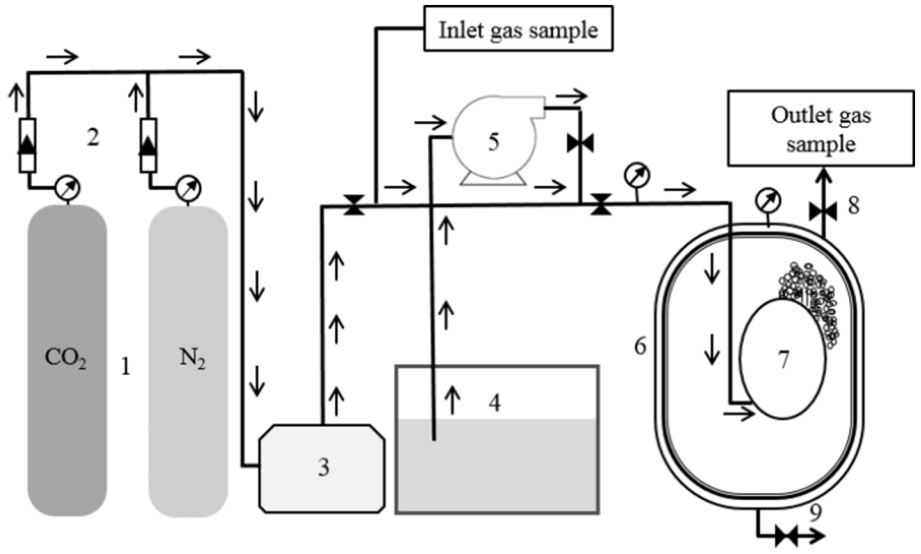

Fig. 1 – Experimental apparatus used for CO_2 absorption: (1) CO_2 and N_2 cylinders; (2) mass flow controllers; (3) mixer; (4) water tank; (5) pump; (6) reactor; (7) liquid-film-forming device; (8) exhaust gas valve; and (9) blowdown valve.

In order to evaluate the absorption rate and the removal efficiency of CO_2, the outlet gas from the exhaust gas valve was collected into a sampling gas bag and then analyzed by gas chromatography (GC-8APT, Shimadzu, Japan). The GC-8APT is equipped with a thermal conductivity detector (TCD) and an activated carbon 60/80 column (1.5 m × 3.0 mm ID). Argon was used as the carrier gas. The operation temperatures for the injector, the column, and the detector were 50, 60, and 50°C, respectively.

The CO_2 concentration in water was measured with a CO_2 meter (CGP-31, DKK-TOA Co., Japan).

According to Pao Chi Chen's study (Chen, 2012), the absorption rate can be calculated by the following formula:

$$R_{CO_2} = \frac{F_{CO_2}}{V}\left[1-\left(\frac{1-x_{CO_2}^{in}}{x_{CO_2}^{in}}\right)\left(\frac{x_{CO_2}^{out}}{1-x_{CO_2}^{out}}\right)\right] = \frac{1}{V}\left(\frac{Q_g P_{CO_2}}{RT}\right)\left[1-\left(\frac{1-x_{CO_2}^{in}}{x_{CO_2}^{in}}\right)\left(\frac{x_{CO_2}^{out}}{1-x_{CO_2}^{out}}\right)\right] \quad (1)$$

where R_{CO_2} (mol/(sec·L)) is the absorption rate of CO_2 in the liquid phase; F_{CO_2} (mol/sec) is the CO_2 molar flow rate; V (L) is the volume of liquid phase in the chamber; ((L/sec) is inlet gas flow rate; P_{CO_2} (atm) is the partial pressure of CO_2; R (L·atm) / (mol·K)) is the constant 0.082; T (K) is the absolute temperature; $x_{CO_2}^{in}$ is the molar fraction of CO_2 at the inlet; and $x_{CO_2}^{out}$ is the molar fraction of CO_2 at the outlet.

1.3. Plackett–Burman design

The Plackett–Burman design (Plackett and Burman, 1946) was used to screen and select the factors significantly affecting CO_2 removal and absorption rate. The four factors investigated were gas pressure (X_1), CO_2 initial concentration (X_2), gas/liquid ratio (X_3), and temperature (X_4). According to the Plackett–Burman design, each parameter was set at two levels: −1 for a low level and +1 for a high level. With these parameters, the program Minitab 14 was used to design the experimental matrix and determine the important factors. The levels of each factor, their values, and their effects as used in the experimental design matrix are given in Table 1. The effect of each parameter was estimated by Eq. (2):

$$E_{X_i} = \frac{2(\sum M_{i+} - M_{i-})}{N} \quad (2)$$

where E_{X_i} is the effect of the tested variables (X_i); M_{i+} and M_{i-} are the responses (CO_2 removal efficiency E and absorption rate R) collected from trials where the variable (X_i) was measured at high and low levels, respectively; and N is the number of experiments.

The factors having a P-value ≤0.1 at the confidence level of 90% were considered as the key factors that acted significantly on the removal rate. These factors were then used in the modeling step utilizing the RSM.

1.4. RSM

After screening the key factors, the next step in the experiment was to determine the model regressions and optimum conditions by using a RSM. The RSM with central composite design (CCD) was employed in this work to evaluate the impact of the independent and significant variables obtained from the Plackett–Burman design: gas pressure (X_1), temperature (X_2), gas/liquid ratio (X_3), and initial CO_2 concentration (X_4). Based on CCD, each parameter was assessed at five coded levels (−2, −1, 0, 1, 2), with the corresponding values enumerated in Table 3. Responses obtained by experiments were represented by quadratic models using the polynomial equation:

$$y = \beta_0 + \sum_{i=1}^{k}\beta_i x_i + \sum_{i=1}^{k}\beta_{ii} x_i^2 + \sum\sum_{i=1}^{k}\beta_{ij} x_i x_j \quad (3)$$

where y is the predicted response; β_0 is the constant; β_i is the linear effect term; β_{ii} is the quadratic effect term; β_{ij} is the interaction effect term; x_i is the variable i; and x_j is the variable j. The quality of fit for the quadratic models was expressed by the

Table 1 – Levels of the experimental variables, estimated effects, and P-value studied in the Plackett–Burman design.

Code	Variable	Low level (−1)	High level (+1)	Removal efficiency [a] E (%)		Absorption rate [b] R × 10^4 (mol/(sec·L))	
				Effect (E_{Xi})	P-value	Effect (E_{Xi})	P-value
X_1	Gas pressure (MPa)	0.50	0.70	5.89 [e]	0.007 [c]	6.74 [e]	0.023 [c]
X_2	CO_2 initial content (%)	15	35	4.25 [e]	0.031 [c]	17.06 [e]	0.000 [c]
X_3	Gas/liquid ratio	0.71	1.43	−15.76 [f]	0.000 [c]	7.37 [e]	0.016 [c]
X_4	Temperature (°C)	10	25	−25.72 [f]	0.000 [c]	−5.07 [f]	0.065 [d]

[a] R^2 = 0.9823; adj R^2 = 0.9721.
[b] R^2 = 0.9172; adj R^2 = 0.8698.
[c] P-value <0.05 (significant at 95% confidence level).
[d] P-value <0.1 (significant at 90% confidence level).
[e] Positive effect.
[f] Negative effect.

coefficient of determination (R^2) and the adjusted coefficient of determination (adj-R^2).

2. Results and discussion

2.1. Screening key factors affecting the removal of CO_2 using tap water as the absorbent

The parameters of gas pressure (X_1), initial CO_2 concentration (X_2), gas/liquid ratio (X_3), and temperature (X_4) were investigated using the Plackett–Burman design to identify how they affected the removal rate *E* and absorption rate *R*. The levels for each factor and the resulting analysis data of estimated effects and probability values (*P*-value) are given in Table 1. The experimental matrix comprising 12 experiments was designed using Minitab 14 software and is given in Table 2. According to the data obtained from Table 1, factors with a *P*-value <0.1 were considered the key factors affecting the removal and absorption rates.

Using a *P*-value <0.1 (with the 90% confidence level), gas pressure and initial CO_2 content exerted significant and positive effects on the removal rate *E*, while the gas/liquid ratio and temperature were found to have a negative influence. Additionally, the parameters of gas pressure, CO_2 initial concentration, and gas/liquid ratio impacted the absorption rate *R* at high rank, with *P*-value <0.05, and showed a positive effect. Only temperature had an inverse and insignificant influence on the absorption rate at the 95% confidence level. However, at the confidence level of 90%, temperature was identified as a significant factor for the response of *R*. Therefore, the four factors of pressure, inlet CO_2 concentration, G/L ratio, and temperature were found to have significant influence on both the removal and absorption rates. Ultimately, gas pressure (X_1), CO_2 initial concentration (X_2), gas/liquid ratio (X_3), and temperature (X_4) were selected for further optimization in the next step using an RSM design.

2.2. Effect of operating factors on the removal of CO_2 using tap water as the absorbent

The 31 experimental trials conducted in this work were targeted to assess the effects of the four variables and construct quadratic models. The experimental matrix, along with the corresponding results of the CCD, is presented in Table 3. The regression equation coefficients were calculated and listed in Table 4. The significance of each coefficient was determined by the Student's *t*-test. In terms of actual units, the responses in removal efficiency *E* (%) and absorption rate

Table 2 – Plackett–Burman design matrix for evaluating influent factors with removal efficiency and absorption rate as responses.

Run	X_1	X_2	X_3	X_4	Removal efficiency *E* (%)		Absorption rate R × 10^4 (mol/(sec·L))	
					Observed	Predicted	Observed	Predicted
1	1	−1	−1	−1	84.74	83.67	11.29	13.28
2	1	1	−1	1	63.12	62.21	25.14	25.28
3	1	1	1	−1	69.34	72.17	44.39	37.71
4	1	1	−1	1	63.05	62.21	25.26	25.28
5	1	−1	1	−1	70.55	67.91	18.62	20.64
6	1	−1	1	1	39.56	42.20	13.06	15.58
7	−1	−1	−1	−1	79.47	77.78	7.85	6.54
8	−1	1	1	−1	65.46	66.27	31.32	30.97
9	−1	−1	−1	1	49.31	52.06	6.64	1.48
10	−1	1	1	1	44.21	40.56	23.35	25.91
11	−1	1	−1	−1	80.27	82.03	19.28	23.61
12	−1	−1	1	1	36.29	36.30	8.91	8.84

Table 3 – Central composite design matrix for the experimental design and predicted responses for removal efficiency *E* (%) and absorption rate *R* (mol/(sec·L)).

Run	Gas pressure (X_1) (MPa)		CO_2 initial content (X_2) (%)		Gas/liquid ratio (X_3)		Temperature (X_4) (°C)		Removal efficiency *E* (%)		Absorption rate $R \times 10^4$ (mol/(sec·L))	
	Actual	Code	Actual	Code	Actual	Code	Actual	Code	Observed	Predicted	Observed	Predicted
1	0.50	0	25	0	1.07	0	30	2	41.30	40.83	13.25	12.13
2	0.50	0	25	0	1.07	0	20	0	52.38	52.17	15.83	15.58
3	0.70	1	15	−1	0.71	−1	25	1	54.40	54.62	9.64	8.68
4	0.50	0	25	0	1.07	0	20	0	51.88	52.17	15.56	15.58
5	0.50	0	25	0	1.07	0	20	0	52.59	52.17	15.88	15.58
6	0.70	1	35	1	0.71	−1	15	−1	78.00	77.41	29.35	30.89
7	0.50	0	10	−2	1.07	0	20	0	50.12	50.90	6.13	6.34
8	0.50	0	25	0	1.07	0	20	0	52.28	52.17	15.76	15.58
9	0.30	−1	35	1	0.71	−1	25	1	64.64	65.55	10.98	11.15
10	0.30	−1	15	−1	1.43	1	15	−1	61.03	61.23	7.70	6.82
11	0.70	1	15	−1	1.43	1	25	1	45.47	44.69	13.06	13.04
12	0.25	−2	25	0	1.07	0	20	0	64.88	63.50	8.98	8.82
13	0.50	0	45	2	1.07	0	20	0	62.71	62.54	32.48	33.10
14	0.70	1	35	1	0.71	−1	25	1	63.08	62.74	25.14	24.90
15	0.70	1	15	−1	1.43	1	15	−1	60.97	59.92	21.07	21.29
16	0.70	1	35	1	1.43	1	15	−1	62.44	62.24	51.31	47.06
17	0.30	−1	35	1	1.43	1	25	1	52.10	52.08	15.67	14.99
18	0.50	0	25	0	1.79	2	20	0	41.90	42.56	18.11	19.81
19	0.70	1	15	−1	0.71	−1	15	−1	73.10	72.98	12.05	11.61
20	0.30	−1	35	1	0.71	−1	15	−1	79.87	80.52	11.64	10.54
21	0.30	−1	15	−1	0.71	−1	15	−1	75.98	75.70	5.04	4.15
22	0.70	1	35	1	1.43	1	25	1	50.54	50.69	34.47	35.75
23	0.30	−1	35	1	1.43	1	15	−1	64.29	63.93	18.36	19.70
24	0.50	0	25	0	1.07	0	10	−2	70.30	71.04	17.90	19.76
25	0.30	−1	15	−1	1.43	1	25	1	45.24	45.70	6.33	5.17
26	0.50	0	25	0	1.07	0	20	0	52.13	52.17	15.70	15.58
27	0.50	0	25	0	1.07	0	20	0	52.48	52.17	15.85	15.58
28	0.50	0	25	0	1.07	0	20	0	52.23	52.17	15.72	15.58
29	0.50	0	25	0	0.36	−2	20	0	69.19	68.79	7.45	6.46
30	0.30	−1	15	−1	0.71	−1	25	1	56.99	57.05	4.71	7.83
31	0.75	2	25	0	1.07	0	20	0	58.85	60.93	24.39	26.45

R (mol/(sec·L)) were fitted with second-order polynomial equations as expressed below:

$$E = 186.21 - 171.32X_1 - 0.54X_2 - 40.90X_3 - 3.98X_4 + 160.65{X_1}^2 + 0.01{X_2}^2 + 7.03{X_3}^2 + 0.04{X_4}^2 - 0.05X_1X_2 + 4.91X_1X_3 + 0.07X_1X_4 - 0.15X_2X_3 + 0.02X_2X_4 + 0.43X_3X_4 \quad (4)$$

$$R \times 10^4 = -8.71 - 30.87X_1 - 0.63X_2 + 11.16X_3 + 1.47X_4 + 32.82{X_1}^2 + 0.01{X_2}^2 - 4.88{X_3}^2 + 1.61X_1X_2 + 24.34X_1X_3 - 1.65X_1X_4 + 0.45X_2X_3 - 0.02X_2X_4 - 0.74X_3X_4 \quad (5)$$

The results of analysis of variance (ANOVA) for the regression models are given in Table 5. The probability values of the regression model in both the *E* and *R* cases equaled 0.000, demonstrating that the models were significant. The high determination coefficients (R^2) of 0.996 and 0.982, together with adjusted determination coefficients (adj R^2) of 0.993 and 0.966, for the responses of removal efficiency and absorption rate, respectively, indicate that the models explained 96.6%–99.6% of the variability in the response variable. Fig. 2 further confirms that there is a good agreement and correlation between the experimental and predicted values of the responses in both models.

The 3D surface plots and contour plots in Figs. 3 and 4 were drawn to clarify the main and interactive effects of the independent variables on the responses. The plots were generated by varying two variables as a function of two significant factors at the same time within the experimental range, while the two other variables were kept constant at the center point.

Figs. 3a and 4a present the interaction effects between gas pressure (X_1) and G/L ratio (X_3) on the removal capacity *E* and absorption rate *R*. In terms of gas pressure, the removal rate fluctuated and reached the lowest point at 0.50 MPa, when pressure was adjusted between 0.25 MPa and 0.75 MPa. Specifically, after a drop in CO_2 removal efficiency that occurred with the rise in pressure from 0.25 to 0.50 MPa, the CO_2 capture increased again when the pressure moved up to 0.75 MPa. Meanwhile, the absorption rate increased steadily with the growth in pressure. Based on Henry's law, pressure normally has a direct influence on the absorption of CO_2 in water, which would explain the strong augmentation in the absorption rate in the pressure range of 0.25 to 0.75 MPa. Interestingly, the CO_2 removal capacity declined with a change in pressure from 0.25 to 0.50 MPa. The reason for this odd behavior is that the increase of pressure leads to an

Table 4 – Significance of regression coefficients for removal efficiency E (%) and absorption rate R (mol/(sec·L)).

Terms	Regression coefficient	Standard error	t-Value	P-value
Removal efficiency E (%)				
Constant	186.207	6.108	30.487	0.000 *
X_1	−171.323	9.811	−17.462	0.000 *
X_2	−0.536	0.163	−3.289	0.005 *
X_3	−40.900	4.333	−9.438	0.000 *
X_4	−3.976	0.337	−11.806	0.000 *
X_1^2	160.650	7.543	21.299	0.000 *
X_2^2	0.012	0.002	6.163	0.000 *
X_3^2	7.031	1.292	5.443	0.000 *
X_4^2	0.038	0.007	5.690	0.000 *
X_1X_2	−0.048	0.111	−0.433	0.671
X_1X_3	4.913	3.085	1.593	0.131
X_1X_4	0.074	0.222	0.332	0.744
X_2X_3	−0.147	0.062	−2.380	0.030 *
X_2X_4	0.018	0.004	4.147	0.001 *
X_3X_4	0.433	0.123	3.506	0.003 *
Absorption rate R (mol/(sec·L))				
Constant	−8.707	12.513	−0.696	0.496
X_1	−30.866	20.100	−1.536	0.144
X_2	−0.625	0.334	−1.872	0.080
X_3	11.164	8.878	1.258	0.227
X_4	1.474	0.690	2.136	0.048 *
X_1^2	32.824	15.452	2.124	0.050 *
X_2^2	0.007	0.004	1.803	0.090
X_3^2	−4.875	2.646	−1.842	0.084
X_4^2	0.004	0.014	0.268	0.792
X_1X_2	1.612	0.228	7.084	0.000 *
X_1X_3	24.34	6.320	3.851	0.001 *
X_1X_4	−1.651	0.455	−3.629	0.002 *
X_2X_3	0.451	0.126	3.568	0.003 *
X_2X_4	−0.015	0.009	−1.687	0.111
X_3X_4	−0.740	0.253	−2.925	0.010 *

* P-value <0.05 (significant at 95% confidence level).

Table 5 – Analysis of variance (ANOVA) for the parameters of central composite design (CCD) for removal efficiency E (%) and absorption rate R (mol/(sec·L)).

Removal efficiency E (%)

Sources of variations	DF	Sum of squares	Mean square	F-value	P-value
Regression	14	3156.97	225.50	285.63	0.000
Linear	4	2614.20	87.08	110.30	0.000
Square	4	512.77	128.19	162.38	0.000
Interaction	6	29.99	5.00	6.33	0.001
Residual error	16	12.63	0.79		
Total	30	3169.60			

Coefficient of determination (R^2) = 0.996

Adjusted determination coefficient (adj R^2) = 0.993

Absorption rate R × 10^4 (mol/(sec·L))

Sources of variations	DF	Sum of squares	Mean square	F-value	P-value
Regression	14	2912.57	208.04	62.79	0.000
Linear	4	2531.14	12.07	3.64	0.027
Square	4	42.42	10.61	3.20	0.041
Interaction	6	339.01	56.50	17.05	0.000
Residual error	16	53.01	3.31		
Total	30	2965.59			

Coefficient of determination (R^2) = 0.982

Adjusted determination coefficient (adj R^2) = 0.966

increase in the gas density as well as the number of CO_2 molecules in each unit of gas volume (Duschek et al., 1990; Wilkinson and Van Dierendonck, 1994; Leonard et al., 2015). This increase leads to a high density of gas in the chamber and prevents contact and mass transfer between the gas phase (CO_2) and liquid phase (water), thus obstructing dissolution of the CO_2 in water.

A decrease in volumetric mass transfer k_La with pressure has also been found in previous research (Teramoto et al., 1974; Maalej et al., 2001; Lee and Foster, 1990; Maalej et al., 2003). Additionally, it has been concluded that the liquid mass transfer coefficient k_L decreased by 20% when pressure increased from 0.10 to 0.40 MPa, and then remained steady at pressures up to 1.0 MPa (Han and Al-Dahhan, 2007; Leonard et al., 2015). Therefore, it is possible to assume that gas–liquid mass transfer and the turbulence of liquid inside the chamber decreases when pressure is elevated to around 0.50 MPa, resulting in higher removal efficacy at 0.25 MPa than at 0.50 MPa. Moreover, because mass transfer remains unchanged at higher pressures (from 0.50 to 0.10 MPa), the effect of mass transfer on the removal rate in the pressure range of 0.50 to 0.75 MPa was negligible. On the other hand, as pressure increases, the mean bubble diameter becomes smaller and the bubbles tend to shrink and collapse further, which then forces the CO_2 in the gas bubbles to dissolve more easily and rapidly into the liquid phase (in this case, water) (Xu et al., 2008). Therefore, the rise of influent gas pressure from 0.50 to 0.75 MPa enabled a growth in the dissolution rate, and therefore led to an increase in the removal rate. Additionally, based on the report of Lovett and Travers, at pressures below 0.50 MPa, the bubble diameter increased with increasing pressure (Lovett and Travers, 1986). This result possibly explains the drop in removal efficiency when increasing the pressure from 0.25 to 0.50 MPa.

The G/L ratio had a negative effect on the removal capacity and a positive effect on the absorption rate. Due to an increase in the inlet gas flow rate from 5 to 25 L/min while keeping the water flow rate at a constant of 14 L/min (equivalent to G/L range of 0.36 to 1.79), a large amount of CO_2 passed through the device and caused a turbulent liquid phase inside the absorption tank, which reduced the contact time between the gas and liquid phase (Chai and Zhao, 2012; Lin and Chu, 2015; Xiao et al., 2014), and ultimately led to a decline in the removal rate. However, according to Eq. (1), a higher gas flow rate stimulates the relative CO_2 molar flow rate per unit of liquid phase, effectively increasing the absorption rate.

The interaction effects between the inlet CO_2 concentration and the gas/liquid flow ratio on CO_2 capture and absorption rate are illustrated in Figs. 3b and 4b, respectively. As shown in these figures, an increase in the inlet CO_2 concentration improves the sequestration of CO_2 into water. At higher initial CO_2 concentrations, the gas partial pressure increased and lowered the resistance between the gas and liquid phases, which caused an accumulation of dissolved CO_2

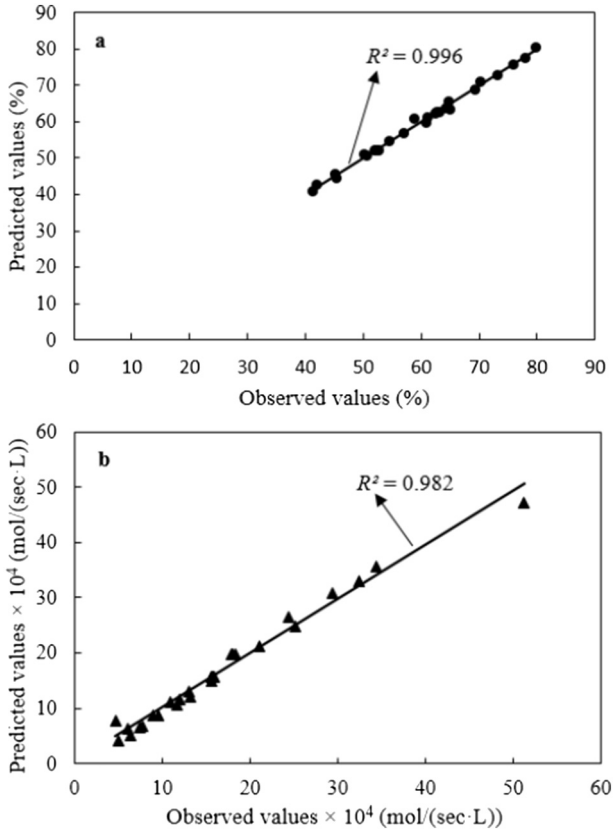

Fig. 2 – Correlation between observed and predicted values for (a) removal efficiency and (b) absorption rate.

in the tap water, as indicated by Henry's law. As a result of this, not only the removal efficiency but also the CO_2 absorption rate improved directly and remarkably with the accumulation of CO_2 when increasing the concentration in the mixed gas from 10% to 45%.

Figs. 3c and 4c illustrate the interactive influences between temperature and pressure. The range of temperature investigated was 10 to 30°C. The solubility of gas is dependent on temperature, and an increase in temperature leads to an increase in the gas dissolution rate (Carroll et al., 1991). Therefore, CO_2 removal efficiency and absorption level decreased with increasing temperature. Furthermore, temperature also had an effect on the bubble diameter, rise velocity, and gas holdup. Increasing temperature resulted in a reduction in the gas holdup and total bubble surface area due to an increase in the bubble rise velocity (Pérez-Garibay et al., 2012). For these reasons, increased temperature had a negative effect on the dissolution rate of CO_2.

2.3. Evaluation of the models and experiment

In order to verify the reliability of our results and to determine the validity of our statistical models and regression equations, 5 additional experiments were conducted under different experimental conditions. The results, including the observed values, predicted values, and % errors between the observed and predicted values for the two responses are listed in Table 6. In each run, the predicted values for removal efficiency and absorption rate calculated from Eqs. (4) and (5), respectively, were compared to the observed values. The % error between predicted and observed values fluctuated in the

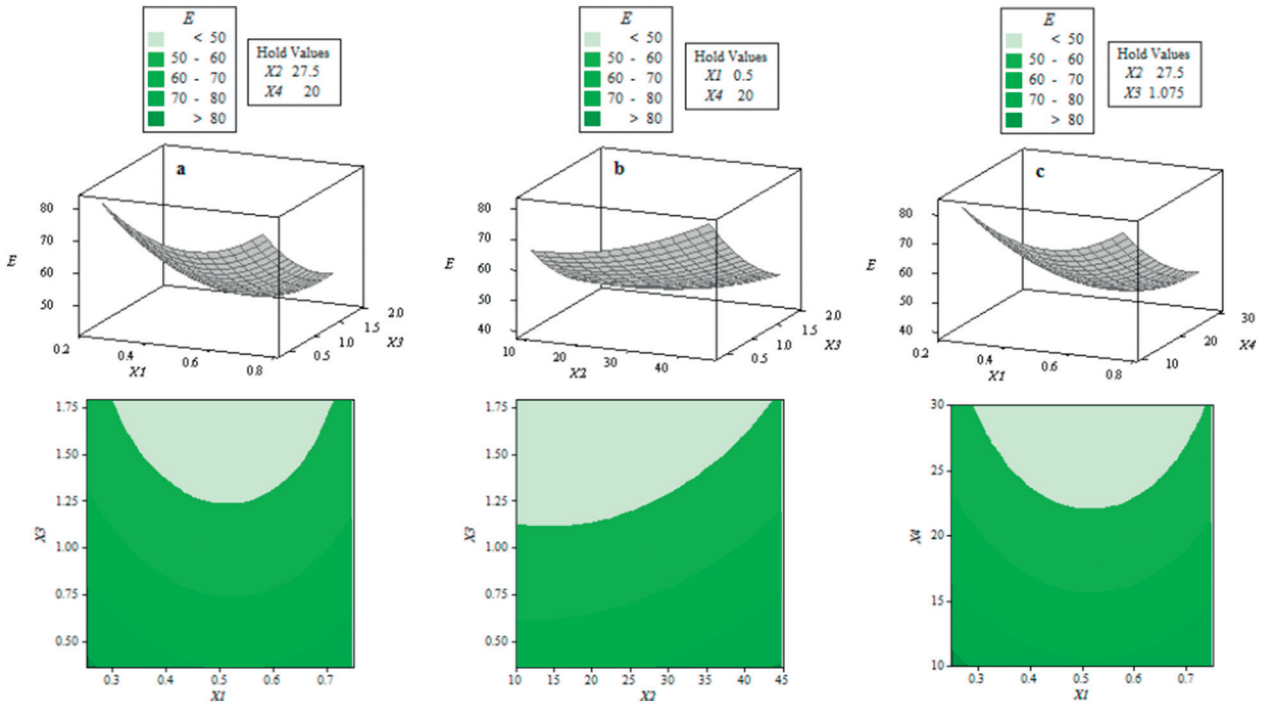

Fig. 3 – Three-dimensional response surface plots and contour plots of removal efficiency interactions between: (a) gas pressure and G/L ratio; (b) CO_2 initial concentration and G/L ratio; (c) gas pressure and temperature.

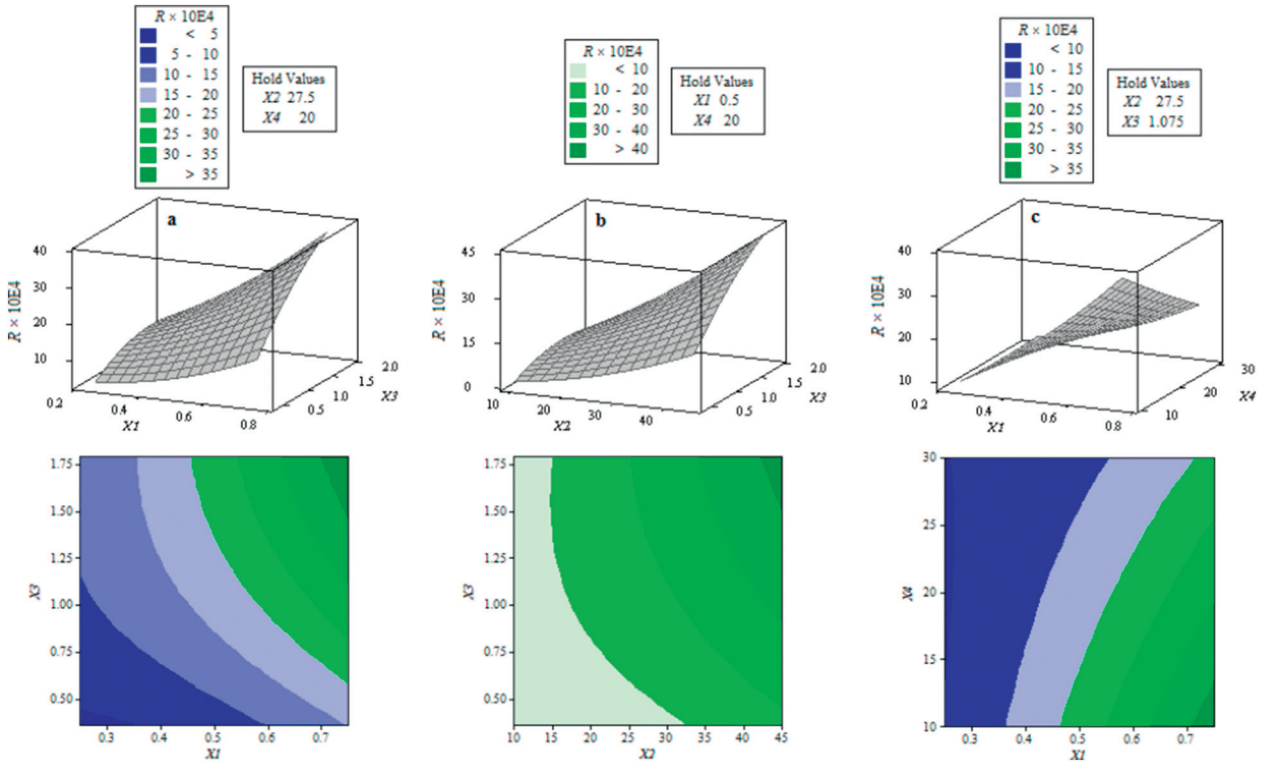

Fig. 4 – Three-dimensional response surface plots and contour plots of absorption rate interaction between: (a) gas pressure and G/L ratio; (b) CO_2 initial concentration and G/L ratio; (c) gas pressure and temperature.

range of 0.46% and 3.69% for the removal efficiency and 3.59% and 8.28% for the absorption rate. The fact that % errors were less than 9% confirmed again that the statistical models obtained from this study are both accurate and reliable. These results, when combined with a high correlation coefficient $R^2 > 0.98$ (shown in Section 2.2), show that the use of the polynomial equations (Eqs. (4) and (5)) to estimate the CO_2 removal efficiency and absorption rate is concise and reliable. With the aid of statistical models and second-order polynomial equations, the CO_2 removal efficiency and absorption rate could be calculated precisely without conducting experiments. Therefore, it is possible to determine the appropriate or optimum conditions for controlling the absorption process to meet the standard requirements of CO_2 removal and absorption rate in a cost effective and timely manner. This approach provides the means to employ this water absorption system in real-time.

Table 7 shows a comparison of the CO_2 removal performance in this study with that of other methods, including conventional water scrubbing (packed column scrubber), amine absorption, adsorption, and membrane techniques. Compared to amine absorption, water scrubbing has some special benefits, *i.e.*, it reduces corrosion problems, it does not release toxic by-products, and the process control is simple. In addition, using water as the absorbent leaves many choices for the disposal of solvents. The disposed water containing high concentrations of CO_2 can also be used for other purposes, such as a carbon source for the cultivation of microalgae (Wang et al., 2008; Singh and Ahluwalia, 2013). Therefore, due to the environmentally friendly advantages, water scrubbing can be considered a better choice for the environment in the comparison with the other technologies (Cozma et al., 2013).

Table 6 – Experimental confirmation for removal efficiency E (%) and absorption rate R (mol/(sec·L)).

Run	Gas pressure (MPa)	CO_2 initial content (%)	Gas/liquid ratio	Temperature (°C)	Removal efficiency E (%)			Absorption rate R × 10^4 (mol/(sec·L))		
					Observed	Predicted	% Error	Observed	Predicted	% Error
1	0.70	25	0.71	15	76.24	73.65	−3.46	18.86	20.49	8.28
2	0.30	15	1.07	20	56.46	58.01	2.71	6.29	6.52	3.59
3	0.30	35	0.71	30	58.24	60.31	−3.49	11.32	10.67	−5.91
4	0.50	35	0.36	10	92.86	93.29	0.46	10.96	11.71	6.61
5	0.50	45	1.43	25	48.92	50.76	3.69	32.14	34.27	6.41

% Error is the percentage of error between observed value and predicted value; $\%\text{Error} = \frac{\text{Predicted value}-\text{Observed value}}{(\text{Predicted value}+\text{Observed value})/2} \times 100\%$.

On the other hand, the disadvantage of conventional water scrubbing is that because water is a weak absorbent, high amounts of energy are required for maintaining the high pressure (1.0–2.0 MPa) required during the absorption process in order to achieve a high mass transfer between the two phases of liquid and gas and high dissolution rate. To solve this problem, this study used tap water as the CO_2 absorbent in the apparatus outfitted with the LFFD to remove carbon dioxide from the gas stream effectively at a low pressure of 0.30 MPa. In the scrubber connected to the LFFD, a large number of liquid-films and fine bubbles were formed, promoting the effective and strong pathway for a high gas transfer efficiency and dissolution rate into water (Imai and Zhu, 2011). Fig. 5 indicates that with the aid of the LFFD, CO_2 dissolved into water faster with a concentration three times higher than in the case of without the LFFD. The reasons for the high CO_2 dissolution rate are that fine bubbles enable large interfacial contact area between the gas and water and have a long residence time in the liquid phase due to their low buoyancy and low slip velocity (Parmar and Majumder, 2013). Therefore, a high CO_2 removal efficiency can be achieved without the use of high pressure. This can be demonstrated by comparison with the results of previous studies. Läntelä et al. (2012) concluded that in an absorption column packed with a pall-ring (4 × 4 cm) filling material for high internal surface area, the removal of CO_2 from the raw landfill gas by water absorption can reach 88.9% under high pressure conditions (2.5 MPa), a CO_2 inlet content of 37.8%–43.6%, a temperature of 10–15°C, and a water flow rate of 11 L/min. Meanwhile, with the aid of a LFFD in enhancing the CO_2 dissolution rate, at the initial conditions of low pressure (0.25 MPa), CO_2 inlet content (40%), temperature (12°C), and gas/liquid ratio (0.71), the water absorption process can achieve a CO_2 removal efficiency of about 92.0%. However, one remaining limitation in this study is the low performance of this process under high gas-to-liquid ratio conditions or a high load of induced gas. This can be explained by the lack of capacity in producing fine bubbles with only one LFFD. Hence, this problem can be solved by increasing the number of LFFDs used in the apparatus. When the number of LFFD increases, the amount of and the speed with which the liquid-films and microbubbles are produced increases. This increase in effectiveness enhances the mass transfer as well as increasing the contact area between the gas and liquid phases, supporting the use of this type of apparatus under conditions with high loads of inlet gas.

3. Conclusions

This study provided evidence that using an RSM in connection with CCD statistical experimental design could successfully construct models identifying the effects of various independent variables, including gas pressure, initial CO_2 concentration, G/L ratio, and temperature, on the CO_2 removal efficiency and the degree of absorption. Good agreements between the predicted values obtained from the two models with the experimentally observed values were achieved, with the coefficient of determination R^2 being more than 0.98 in both cases. The models can be used as useful tools to predict the CO_2 removal efficiency and absorption rate accurately without carrying out a large number of experiments.

In order to achieve high efficiency of CO_2 capture from the mixed gas, the water scrubbing process was designed with gas pressure set under 0.30 MPa or over 0.70 MPa. However, for the aim of reducing operating cost, the lower the gas pressure,

Table 7 – Comparison of different CO_2 removal technologies.

Parameter	This study	Conventional water scrubbing	Amine absorption	Adsorption	Membrane
Working pressure	<0.30 MPa	1.0–2.0 MPa [a]	Low pressure [a]	0.7–0.8 MPa (pressure swing adsorption) [g]	2.5–4.0 MPa [a]
Operation and maintain cost	Low	Low [d,g]	High [f]	High [g]	High membrane cost [a]
Energy requirement	1.5–4.5 MJ/kgCO_2	–	4–6 MJ/kgCO_2 [c]	2 – 3 MJ/kgCO_2 [c]	0.5–6 MJ/kgCO_2 [c]
Toxic by-product	Low	Low [d]	High [b,f]	Low [a,f]	Low [c,f]
Corrosion rate	Moderate	Moderate [a]	High [a,b,e]	Low [a]	Low [e]
Control requirement	Low	–	High [c]	High [c]	Low [c]
Other	Less environmental impact because no chemical is required in the scrubbing process. However, the process is slow and requires a lot of water [a,d].		High environmental impact due to sorbent degradation, generation of volatile degradation compounds and the disposal of solvent [b].	High temperature is required in the adsorption process [b].	Operational problems include low flux and fouling [b].

List of references used in Table 7.
[a] Andriani et al. (2014).
[b] Leung et al. (2014).
[c] Mondal et al. (2012).
[d] Ofori-Boateng and Kwofie (2009).
[e] Olajire (2010).
[f] Shimekit and Mukhtar (2012).
[g] Zhao et al. (2010).

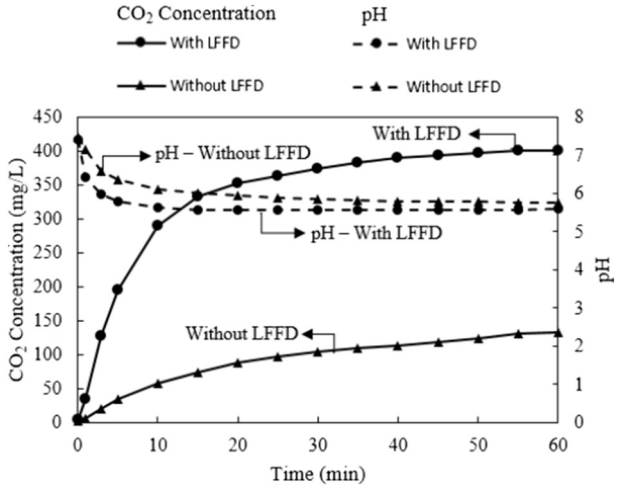

Fig. 5 – CO_2 concentration dissolving into 60 L of water and the change of pH during 60 min in two cases of with and without using liquid-film-forming device (LFFD). Inlet gas pressure: 0.50 MPa; inlet gas composition: 15% CO_2–85% N_2; G/L ratio: 1.43; and temperature: 20°C.

the lower expenditure is. In addition, higher inlet CO_2 concentrations, lower temperatures, and lower G/L ratios improved the solubility of CO_2 in water. However, due to the low G/L ratio, the absorption rate of the absorption process was low, and was thus uneconomical. Accordingly, to achieve not only a high removal rate but also a satisfactory absorption rate, it is suggested to consider the mass flow of the feed gas, efficacy demand, and required CO_2 separation process before selecting the optimal conditions. Eventually, further research will be needed to further develop an apparatus design for connecting several liquid-film generators, which is expected to enable not only a high removal rate but also a great absorption rate. In future studies, measurements of the bubble sizes and mass transfer coefficients will be carried out to comprehensively assess the absorption process.

Acknowledgments

The authors gratefully acknowledge the support of the Ministry of Education, Culture, Sports, Science, and Technology of Japan (MEXT – Monbukagakusho Scholarship) and Yashima Environment Technology Foundation. We also would like to thank all of our colleagues in the Division of Environmental Science and Engineering — Yamaguchi University, Japan for their help and valued consideration.

REFERENCES

Andriani, D., Wresta, A., Atmaja, T.D., Saepudin, A., 2014. A review on optimization production and upgrading biogas through CO_2 removal using various techniques. Appl. Biochem. Biotechnol. 172 (4), 1909–1928.

Aresta, M., 2013. Carbon Dioxide Recovery and Utilization. Springer Sci. & Business Media, Germany.

Babu, P.V., 2014. Hydrate Based Gas Separation (HBGS) Technology for Precombustion Capture of Carbon Dioxide. (PhD thesis). National University of Singapore, Singapore.

Bang, J.-H., Kim, W., Song, K.S., Jeon, C.W., Chae, S.C., Cho, H.-J., Jang, Y.N., Park, S.-J., 2014. Effect of experimental parameters on the carbonate mineralization with $CaSO_4{\cdot}2H_2O$ using CO_2 microbubbles. Chem. Eng. J. 244, 282–287.

Carroll, J.J., Slupsky, J.D., Mather, A.E., 1991. The solubility of carbon dioxide in water at low pressure. J. Phys. Chem. Ref. Data 20 (6), 1201–1209.

Chai, X., Zhao, X., 2012. Enhanced removal of carbon dioxide and alleviation of dissolved oxygen accumulation in photobioreactor with bubble tank. Bioresour. Technol. 116, 360–365.

Chen, P.-C., 2012. Absorption of Carbon Dioxide in a Bubble-Column Scrubber. INTECH Open Access Publisher.

Chou, C., 2013. Carbon dioxide separation and capture for global warming mitigation. J. Adv. Eng. Technol. 1, 1–4.

Cozma, P., Ghinea, C., Mămăligă, I., Wukovits, W., Friedl, A., Gavrilescu, M., 2013. Environmental impact assessment of high pressure water scrubbing biogas upgrading technology. Clean: Soil, Air, Water 41 (9), 917–927.

Duschek, W., Kleinrahm, R., Wagner, W., 1990. Measurement and correlation of the (pressure, density, temperature) relation of carbon dioxide I. The homogeneous gas and liquid regions in the temperature range from 217K to 340K at pressures up to 9 MPa. J. Chem. Thermodyn. 22 (9), 827–840.

Han, L., Al-Dahhan, M.H., 2007. Gas–liquid mass transfer in a high pressure bubble column reactor with different sparger designs. Chem. Eng. Sci. 62 (1), 131–139.

Imai, T., Zhu, H., 2011. Improvement of Oxygen Transfer Efficiency in Diffused Aeration Systems Using Liquid-Film-Forming Apparatus. INTECH Open Access Publisher.

Läntelä, J., Rasi, S., Lehtinen, J., Rintala, J., 2012. Landfill gas upgrading with pilot-scale water scrubber: performance assessment with absorption water recycling. Appl. Energy 92, 307–314.

Lee, J., Foster, N., 1990. Measurement of gas–liquid mass transfer in multi-phase reactors. Appl. Catal. 63 (1), 1–36.

Lee, Z.H., Lee, K.T., Bhatia, S., Mohamed, A.R., 2012. Post-combustion carbon dioxide capture: evolution towards utilization of nanomaterials. Renew. Sustain. Energy Rev. 16 (5), 2599–2609.

Leonard, C., Ferrasse, J.-H., Boutin, O., Lefevre, S., Viand, A., 2015. Bubble column reactors for high pressures and high temperatures operation. Chem. Eng. Res. Des. 100, 391–421.

Leung, D.Y., Caramanna, G., Maroto-Valer, M.M., 2014. An overview of current status of carbon dioxide capture and storage technologies. Renew. Sustain. Energy Rev. 39, 426–443.

Li, B., Duan, Y., Luebke, D., Morreale, B., 2013. Advances in CO_2 capture technology: a patent review. Appl. Energy 102, 1439–1447.

Lin, C.-C., Chu, C.-R., 2015. Feasibility of carbon dioxide absorption by NaOH solution in a rotating packed bed with blade packings. Int. J. Greenhouse Gas Control 42, 117–123.

Lovett, D., Travers, S., 1986. Dissolved air flotation for abattoir wastewater. Water Res. 20 (4), 421–426.

Maalej, S., Benadda, B., Otterbein, M., 2001. Influence of pressure on the hydrodynamics and mass transfer parameters of an agitated bubble reactor. Chem. Eng. Technol. 24 (1), 77–84.

Maalej, S., Benadda, B., Otterbein, M., 2003. Interfacial area and volumetric mass transfer coefficient in a bubble reactor at elevated pressures. Chem. Eng. Sci. 58 (11), 2365–2376.

Ma'mun, S., Svendsen, H.F., Hoff, K.A., Juliussen, O., 2007. Selection of new absorbents for carbon dioxide capture. Energy Convers. Manag. 48 (1), 251–258.

Mondal, M.K., Balsora, H.K., Varshney, P., 2012. Progress and trends in CO_2 capture/separation technologies: a review. Energy 46 (1), 431–441.

Moreira, D., Pires, J.C.M., 2016. Atmospheric CO_2 capture by algae: negative carbon dioxide emission path. Bioresour. Technol. 215, 371–379.
Ofori-Boateng, C., Kwofie, E., 2009. Water scrubbing: a better option for biogas purification for effective storage. World Appl. Sci. J. 5 (3), 122–125.
Olajire, A.A., 2010. CO_2 capture and separation technologies for end-of-pipe applications — a review. Energy 35 (6), 2610–2628.
Parmar, R., Majumder, S.K., 2013. Microbubble generation and microbubble-aided transport process intensification — a state-of-the-art report. Chem. Eng. Process. Process Intensif. 64, 79–97.
Pérez-Garibay, R., Martínez-Ramos, E., Rubio, J., 2012. Gas dispersion measurements in microbubble flotation systems. Miner. Eng. 26, 34–40.
Plackett, R.L., Burman, J.P., 1946. The design of optimum multi-factorial experiments. Biometrika 33, 305–325.
Rao, A.B., Rubin, E.S., 2002. A technical, economic, and environmental assessment of amine-based CO_2 capture technology for power plant greenhouse gas control. Environ. Sci. Technol. 36 (20), 4467–4475.
Shimekit, B., Mukhtar, H., 2012. Natural Gas Purification Technologies-Major Advances for CO_2 Separation and Future Directions. INTECH Open Access Publisher Croatia, Europe.
Singh, U.B., Ahluwalia, A.S., 2013. Microalgae: a promising tool for carbon sequestration. Mitig. Adapt. Strateg. Glob. Chang. 18 (1), 73–95.
Teramoto, M., Tai, S., Nishii, K., Teranishi, H., 1974. Effects of pressure on liquid-phase mass transfer coefficients. Chem. Eng. J. 8 (3), 223–226.
Wang, B., Li, Y., Wu, N., Lan, C.Q., 2008. CO_2 bio-mitigation using microalgae. Appl. Microbiol. Biotechnol. 79 (5), 707–718.
Weiss, R.F., 1974. Carbon dioxide in water and seawater: the solubility of a non-ideal gas. Mar. Chem. 2 (3), 203–215.
Wilkinson, P.M., Van Dierendonck, L.L., 1994. A theoretical model for the influence of gas properties and pressure on single-bubble formation at an orifice. Chem. Eng. Sci. 49 (9), 1429–1438.
Xiao, Y., Yuan, H., Pang, Y., Chen, S., Zhu, B., Zou, D., Ma, J., Yu, L., Li, X., 2014. CO_2 removal from biogas by water washing system. Chin. J. Chem. Eng. 22 (8), 950–953.
Xu, Q., Nakajima, M., Ichikawa, S., Nakamura, N., Shiina, T., 2008. A comparative study of microbubble generation by mechanical agitation and sonication. Innovative Food Sci. Emerg. Technol. 9 (4), 489–494.
Yu, C.-H., Huang, C.-H., Tan, C.-S., 2012. A review of CO_2 capture by absorption and adsorption. Aerosol Air Qual. Res. 12 (5), 745–769.
Zhao, Q., Leonhardt, E., MacConnell, C., Frear, C., Chen, S., 2010. Purification Technologies for Biogas Generated by Anaerobic Digestion. Compressed Biomethane. CSANR, Ed.